BMC Cancer

RESEARCH Open Access

Camrelizumab combined with apatinib plus irinotecan as a second-line treatment in advanced or metastatic esophageal squamous cell carcinoma patients

Shusheng Wu[1,2], Huiqin Luo[1,2], Wenju Chen[1,2], Xudong Liu[3], Huimin Li[1,2], Mengge Li[1,2], Lihong Ke[1,2], Jiayu Niu[1,2], Bing Hu[1], Huijun Xu[1], Gang Wang[1,2], Ying Yan[1,2], Lulu Cao[1,2], Xiaoxiu Hu[1,2], Chenghui Li[4] and Yifu He[1,2*]

Abstract

Background Camrelizumab (CAM) combined with apatinib plus chemotherapy as a first-line treatment shows good efficacy in advanced or metastatic esophageal squamous cell carcinoma (ESCC) patients. This study aimed to explore the potential of CAM combined with apatinib plus irinotecan (IRT) as a second-line treatment in advanced or metastatic ESCC patients.

Methods A total of 59 advanced or metastatic ESCC patients receiving CAM combined with apatinib plus IRT as second-line treatment were enrolled in this study between January 2020 and March 2024. The primary endpoint was progression-free survival (PFS), with secondary endpoints including overall survival (OS), the objective response rate (ORR), the disease control rate (DCR), and the assessment of toxicity. Concurrently, a model was constructed utilizing patients' clinical characteristics and radiomic features to predict the patients' prognoses.

Results At the time of analysis, 58 patients were withdrawn due to disease progression ($n=9$), death ($n=43$), or lost to follow-up ($n=6$), and 1 patient was ongoing. The ORR and DCR were 37.7% and 84.9%, respectively. The median PFS and OS were 6.3 (95% CI: 4.8–7.8) and 16.7 (95% CI: 13.5–19.9) months, respectively. The most common adverse events of any grade were leukopenia (52.5%), fatigue (25.4%), anemia (23.7%), thrombocytopenia (23.7%), neutropenia (22.0%), and hypoalbuminemia (22.0%). Most of the adverse events were grade I-II. The incidence of grade III-IV adverse events was 20.3%. Predictive models were established based on the outcomes of multivariate Cox analyses. The combined model had an excellent ability to predict the 1-year OS [AUC (95% CI): 0.979 (0.930-1.000)].

Conclusion CAM combined with apatinib plus IRT as a second-line treatment exhibits acceptable efficacy and safety in advanced or metastatic ESCC patients. The model that combines clinical and radiomic features has the greatest ability to predict the survival of advanced or metastatic ESCC patients.

Keywords Advanced or metastatic esophageal squamous cell carcinoma, Camrelizumab, Apatinib, Second-line treatment, Predictive models

*Correspondence:
Yifu He
yifuhe@fsyy.ustc.edu.cn

Full list of author information is available at the end of the article

Introduction

Esophageal squamous cell carcinoma (ESCC) is the most common subtype of esophageal cancer, accounting for more than 80% of all esophageal cancer cases [1]. Most ESCC patients are diagnosed at an advanced stage, and the first-line treatment for these patients is platin/fluoropyrimidine-based chemotherapy with or without immunotherapy [2, 3]. Once first-line treatment fails, the choice of second-line treatment for advanced or metastatic ESCC patients is limited, which mainly involves chemotherapy, such as irinotecan (IRT) monotherapy [2, 4]. Therefore, exploring alternative second-line treatments is crucial for advanced or metastatic ESCC patients.

Targeted therapy, such as apatinib, has made advancements in managing advanced ESCC [5, 6]. Apatinib exerts its effects by specifically inhibiting the tyrosine kinase activity of vascular endothelial growth factor receptor-2, thereby suppressing tumor angiogenesis [7]. Some studies have reported that second- or subsequent-line apatinib shows satisfactory efficacy and safety in advanced ESCC patients [8–10]. Recently, apatinib has been used in combination with immunotherapy as a second-line treatment in patients with digestive cancers, benefiting from their synergistic antitumor effect [11].

Camrelizumab (CAM), an immune checkpoint inhibitor, acts by blocking the interaction between programmed cell death-1 and its ligands, thereby promoting the activity of T cells and enhancing the immune response against tumors [12]. A previous study reported the efficacy and safety of CAM plus apatinib and chemotherapy as the first-line treatment in advanced ESCC patients [13]. This study revealed that CAM plus apatinib, liposomal paclitaxel, and nedaplatin as the first-line treatment achieved an objective response rate (ORR) and disease control rate (DCR) of 80.0% and 96.7%, respectively, in advanced ESCC patients, with the most frequent adverse events of reactive capillary hemangiomas, alopecia, increased alanine aminotransferase (ALT) levels, thrombocytopenia, and anemia [13]. However, the potential of CAM plus apatinib and chemotherapy as the second-line treatment for advanced or metastatic ESCC patients remains unclear.

Accordingly, the current study aimed to explore the efficacy and safety of CAM combined with apatinib plus IRT as a second-line treatment in advanced or metastatic ESCC patients.

Methods

Patients

In this single-arm, open-label, phase 2 study, 59 patients diagnosed with advanced or metastatic ESCC were enrolled between January 2020 and March 2024. The eligibility criteria were as follows: (1) aged greater than 18 years, male or female; (2) diagnosis of advanced or metastatic ESCC by histopathology or cytology; (3) measurable lesions complying with RECIST 1.1 criteria; (4) previous systemic first-line chemotherapy failed or intolerable; (5) physical performance score Eastern Cooperative Oncology Group performance status (ECOG PS) 0–1; (6) no serious hematopoietic function, heart, lung, liver, or kidney function abnormalities or immune deficiency; laboratory tests met the following requirements: neutrophils $\geq 1.5 \times 10^{\wedge}9$/L; hemoglobin ≥ 9 g/dL; platelets $\geq 100 \times 10^{\wedge}9$/L; total bilirubin (TBIL) ≤ 1.5 times the upper limit of normal value; aspartate aminotransferase (AST) (SGOT) and ALT (SGPT) ≤ 2.5 times the upper limit of normal value; creatinine (Cr) ≤ 1.5 times the upper limit of normal value; (7) subjects voluntarily joined the study, signed informed consent, good compliance, and cooperated with follow-up; (8) researchers believed that treatment can benefit. Patients were excluded if (1) the primary esophageal cancer had a risk of perforating and bleeding, which invaded the trachea or adjacent large blood vessels or the heart; (2) patients who had been proven to be allergic to the test drug and its accessories; (3) the subject had an active immune disease or history, had a history of organ transplantation; (4) subjects were being treated with immunosuppressive agents, or systemic or absorbable local hormones for immunosuppressive purposes (dose > 10 mg/day prednisone or other curative hormones), and enrolled continued use within the first 2 weeks, except for the use of toxic hormones produced by radiotherapy and chemotherapy; (5) had clinical symptoms or diseases of the heart that were not well controlled, such as: (1) heart failure above New York Heart Association (NYHA) level 2; (2) not stable angina pectoris; (3) myocardial infarction occurred within 1 year; 6) pregnant or lactating women; 7) patients who were unsuitable for inclusion in the study at the judgment of the investigator. The study was approved by the Medical Ethics Committee of the First Affiliated Hospital of USTC West District (Approval Number: Lunshen 2019 No. 24) and was prospectively registered in the China Clinical Trial Registry (ChiCTR2000028857) on January 5, 2020. Informed consent was obtained from all patients.

Trial design and treatment

CAM (200 mg) was administered intravenously on day (D) 1. IRT was administered intravenously at 60 mg/m^2 at D1 and D8. Apatinib (250 mg) was administered orally from D1 to D21. The treatment was administered for 4–6 cycles in a 21-day cycle. CAM and apatinib were maintained until disease progression or unacceptable toxicity. The dosages of apatinib and IRT could be adjusted on the basis of the patient's condition. Tumor response was evaluated via RECIST 1.1 every 4 weeks for the first

6 months and then every 12 weeks until disease progression. The median (range) follow-up time was 15.3 (1.4–54.9) months.

Endpoints

The primary endpoint of this study was progression-free survival (PFS) in all assigned patients. The secondary endpoints included overall survival (OS), the ORR, the DCR, and safety and tolerability. PFS was defined as the length of time from treatment initiation to disease progression or any-cause death. OS was defined as the length of time from treatment initiation to any-cause death. The ORR and DCR were evaluated as follows: the ORR was defined as the best overall response of complete response (CR) + partial response (PR) rates, and the DCR was defined as the best overall response of CR + PR + stable disease (SD) rates.

Clinical characteristics collection

Patient characteristics, which included age, sex, body mass index (BMI), disease-related history, ECOG PS, tumor-node-metastasis (TNM) stage, tumor size, tumor location, number of metastatic sites, location of metastases, distant metastases, tumor differentiation, and serum test information, were collected. Information on disease progression and survival was also collected, and according to the corresponding time-period information, accumulating progression-free survival (PFS) rate and accumulating overall survival (OS) rate were determined. In addition, adverse events were recorded and evaluated via the National Cancer Institute Common Terminology Criteria for Adverse Events (version 5.0).

Feature extraction

The enhanced computed tomography (CT) images were imported into ITK-SNAP (www.itk-snap.org), where the target lesion margins were delineated layer-by-layer on arterial-phase CT images, forming a three-dimensional region of interest. Two radiologists, each with over 15 years of clinical diagnostic experience, independently reviewed the images to ensure repeatability in both intra- and inter-observer segmentation. Intra- and inter-observer consistency of feature extraction was evaluated using intraclass correlation coefficients (ICCs). To calculate intra-observer ICC, 15 randomly selected CT images were segmented twice by Reader A over a one-month period (with intervals of at least 10 days). For inter-observer ICC calculation, the selected images were segmented independently by two radiologists (Reader A and Reader B). Segmentation was conducted to enable independent feature extraction, allowing for the calculation of both intra- and inter-observer ICC. An ICC greater than 0.75 was considered to indicate good consistency, with the remaining segmentations performed by Reader A. Radiomic features of esophageal lesions were extracted via the PyRadiomics software package (http://pyradiomics.readthedocs.io) based on Python, in alignment with the Imaging Biomarker Standardization Initiative guidelines. The Radiomics Documentation (https://pyradiomics.readthedocs.io/en/latest/index.Html) provided detailed descriptions of these radiomic features. Feature selection was conducted via R software v. 4.3.2 (The R Foundation for Statistical Computing, Vienna, Austria). Z score normalization was applied to unify the scales of different features, ensuring that outdated feature scales fell within a range of 0 to 1. To eliminate redundant radiomic features, pairwise correlation analysis was performed via the "findCorrelation" function in the "caret" package in R, with an absolute correlation cutoff of 0.9. The least absolute shrinkage and selection operator (LASSO) Cox regression model—a method suitable for high-dimensional predictor regression that penalized and shrank some regression coefficients to zero—was used to select the most predictive radiomic features. The penalty parameter (lambda) was determined through ten-fold cross-validation based on the minimum error criterion.

Model development and evaluation

The selected features were weighted based on the basis of their respective coefficients obtained from the LASSO model, and the Rad score was calculated via a linear combination of these weighted features. The cutoff value for the Rad score was determined via X-tile software (version 3.6.1; Yale University School of Medicine, New Haven, USA). Based on this cutoff, patients were categorized into high-risk and low-risk groups, and the Kaplan-Meier method was applied to compare survival differences between these groups, providing an initial assessment of the association between the radiomics model and OS. Previous studies demonstrated that combining radiomic features with high predictive potential yielded better performance than using individual features alone [14]. Therefore, in accordance with prior research, multivariate Cox proportional hazards models were used to select radiomic features with significant predictive value ($P < 0.05$) for subsequent model construction [15, 16]. The selected radiomic features were incorporated into a multivariable Cox proportional hazards model based on clinical characteristics, identifying independent prognostic factors that include both radiomic and clinical features. Nomograms and calibration curves were constructed based on the clinical, radiomic, and combined features. To evaluate the predictive value of these three models for patient prognosis, we used time-dependent receiver operating characteristic (ROC) curves and the concordance index (C-index). Additionally, we assessed the net benefits of the three models via decision curve analysis (DCA).

Sample size calculation

The sample size was calculated using G*Power (version 3.1.9.7). A one-sided exact binomial test was used to assess whether the ORR of the investigational treatment exceeded a predefined historical control. The null hypothesis response rate was set at 34.6% [17], and the expected ORR was assumed to be 55.0%. With a one-sided significance level (α) of 0.05 and a power (1 – β) of 0.90, the required sample size was estimated to be 53 patients, achieving an actual power of 90.0%. Considering the 10% drop off rate, the final estimated sample size was 59.

Statistics

The analysis of this study was based on the full analysis set. SPSS (version 29.0, IBM, USA) was used for data analysis. Descriptive statistics were used to describe the clinical characteristics, best overall response, and adverse events of advanced or metastatic ESCC patients. A Kaplan–Meier curve was used to display the accumulating PFS and accumulating OS rates. The full plot of the best change in tumor size from baseline was generated with R software version 4.3.3, in which the 'dplyr' library was used. Univariable and multivariable Cox regression analyses were used to explore factors related to PFS and OS. We used the "glmnet" package to perform LASSO Cox regression. The "rms" package was used for multivariate Cox regression analysis, nomogram construction, and calibration. The "DynNom" package was used to construct nomograms on the web. The R function cox.zph was employed to test the proportional hazards assumption for a Cox regression model fit. The C-index was calculated and compared via function concordance. index and C-index. comp in the "survcomp" package. Prediction error curves were generated via the "pec" package. A P value < 0.05 indicated statistical significance.

Results

Patients and treatment

A total of 64 advanced or metastatic ESCC patients were recruited, and 5 patients were initially excluded because they did not receive the treatment regimen specified in this study ($n = 1$) or had incomplete baseline CT scans ($n = 4$). A total of 59 patients were enrolled in this study. Among these patients, 58 of them were withdrawn due to disease progression ($n = 9$), death ($n = 43$), and lost to follow-up ($n = 6$). Only 1 patient was ongoing (Fig. 1).

Baseline characteristics

The median [interquartile range (IQR)] age of the patients was 67.0 (59.0–71.0) years. In terms of sex, 8 (13.6%) patients were female, and 51 (86.4%) patients were male. Four (6.8%) patients had an ECOG PS score of 0, and 55 (93.2%) patients had an ECOG PS score of 1. The median (IQR) tumor size was 30.0 (19.0–43.0) mm. Thirty-nine (66.1%), 15 (25.4%), 3 (5.1%), and 2 (3.4%) patients had 1, 2, 3, and 4 metastatic sites, respectively. There were 15 (25.4%), 8 (13.6%), 53 (89.8%), and 9 (15.3%) patients with metastases in the liver, lung, lymph node, and other locations, respectively. A total of 47 (79.7%) patients had distant metastasis. The detailed clinical characteristics are shown in Table 1.

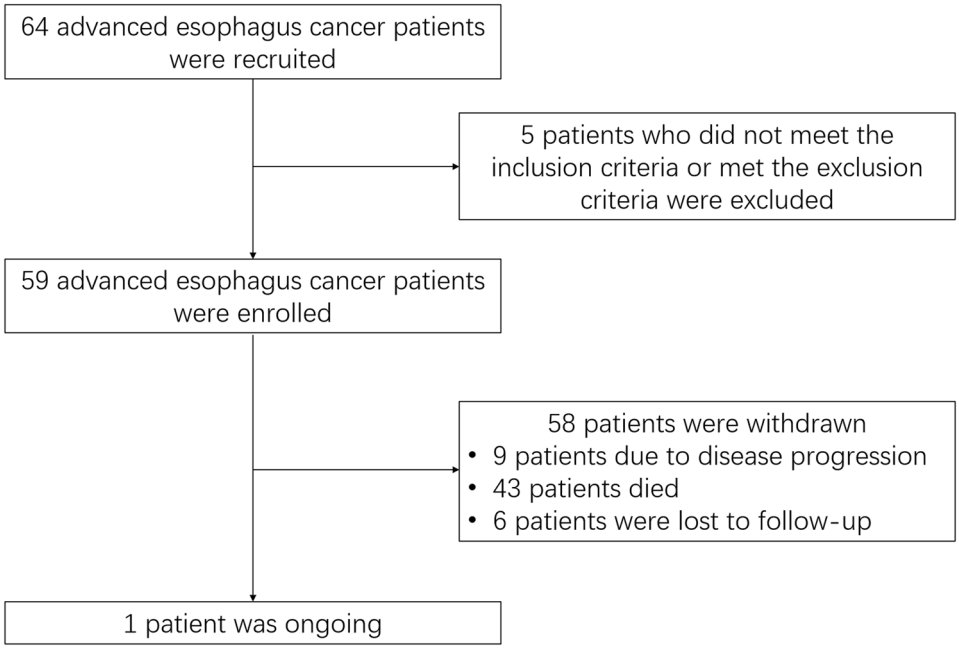

Fig. 1 Patient screening and analysis flow diagram

Table 1 Clinical characteristics of patients with advanced ESCC

Characteristics	Patients (*N* = 59)
Age (years), median (IQR)	67.0 (59.0–71.0)
Age stratification, n (%)	
< 65 years	21 (35.6)
≥ 65 years	38 (64.4)
Sex, n (%)	
Female	8 (13.6)
Male	51 (86.4)
BMI (kg/m^2), mean ± SD	21.1 ± 3.3
History of surgery related to primary lesion, n (%)	32 (54.2)
History of radiotherapy, n (%)	23 (39.0)
History of systemic chemotherapy, n (%)	59 (100.0)
History of targeted therapy, n (%)	4 (6.8)
ECOG PS, n (%)	
0	4 (6.8)
1	55 (93.2)
Tumor location, n (%)	
Cervical esophagus	8 (13.6)
Thoracic esophagus	48 (81.4)
Abdominal esophagus	3 (5.1)
Tumor size (mm), median (IQR)	30.0 (19.0–43.0)
TNM stage, n (%)	
IV	59 (100.0)
Number of metastatic sites, n (%)	
1	39 (66.1)
2	15 (25.4)
3	3 (5.1)
4	2 (3.4)
Location of metastases, n (%)	
Liver	15 (25.4)
Lung	8 (13.6)
Lymph node	53 (89.8)
Other	9 (15.3)
Distant metastases, n (%)	47 (79.7)
Tumor differentiation, n (%)	
Well	1 (1.7)
Moderately	27 (45.8)
Moderately-to-poorly	3 (5.1)
Poorly	19 (32.2)
Undifferentiated	9 (15.3)
CEA (ng/mL), median (IQR)	2.8 (1.8–4.7)
TBIL (μmol/L), median (IQR)	8.5 (6.8–12.9)
DBIL (μmol/L), median (IQR)	3.9 (2.9–4.9)
IBIL (μmol/L), median (IQR)	5.0 (3.8–8.2)
ALT (U/L), median (IQR)	12.5 (9.0-18.3)
AST (U/L), median (IQR)	17.5 (14.0–23.0)
ALP (U/L), median (IQR)	89.0 (68.8-110.3)
GGT (U/L), median (IQR)	24.0 (16.0–39.0)
LDH (U/L), median (IQR)	181.0 (153.3-219.3)
ALB (g/L), mean ± SD	39.3 ± 4.6
BUN (mmol/L), median (IQR)	5.4 (4.4–6.5)
Cr (μmol/L), mean ± SD	73.1 ± 16.0
UA (μmol/L), mean ± SD	325.7 ± 100.6

ESCC, esophageal squamous cell carcinoma; IQR, interquartile range; BMI, body mass index; SD, standard deviation; ECOG PS, Eastern Cooperative Oncology Group Performance Status; TNM, tumor-node-metastasis; CEA, carcinoembryonic antigen; TBIL, total bilirubin; DBIL, direct bilirubin; IBIL, indirect bilirubin; ALT, alanine aminotransferase; AST, aspartate aminotransferase; ALP, alkaline phosphate; GGT, gamma-glutamyl transferase; LDH, lactic dehydrogenase; ALB, albumin; BUN, urea nitrogen; Cr, creatinine; UA, uric acid. Special illustration: All the continuous variables were completed abnormal distribution test by the Kolmogorov-Smirnov test. Non-normal distribution variables were described as median (IQR), and normal distribution variables were described as mean ± SD

Efficacy

A total of 53 patients with clinical response data were included in the treatment response analysis. CR, PR, SD, and progressive disease (PD) rates were 1.9%, 35.8%, 47.2%, and 15.1%, respectively. The ORR and DCR were 37.7% and 84.9%, respectively (Fig. 2A). Figure 2B shows the best target lesion diameter change from baseline in each patient. Thirty-three patients experienced target lesion diameter reduction from baseline, and 20 of them had the best target lesion diameter reduction from baseline > 30%.

In patients who achieved CR, the times of first confirmed PR and CR were 1.8 and 7.7 months, respectively, after second-line treatment with CAM combined with apatinib plus IRT. In those who achieved a PR, the median (IQR) time of the first confirmed PR was 1.9 (1.6–2.4) months after the second-line treatment (Fig. 3).

The median PFS [95% confidence interval (CI)] was 6.3 (4.8–7.8) months. The 6-, 12-, 18-, 24-, 30-, and 36-month accumulating PFS rates were 50.9%, 17.0%, 5.7%, 5.7%, 3.8%, and 1.9%, respectively (Fig. 4A). The median OS (95% CI) was 16.7 (13.5–19.9) months. The 6-, 12-, 18-, 24-, 30-, 36-, 42-, 48-, and 54-month accumulating OS rates were 88.7%, 65.2%, 47.1%, 28.2%, 5.6%, 5.6%, 5.6%, 5.6%, and 5.6%, respectively (Fig. 4B).

Safety profiles

The most common adverse events of any grade were leukopenia (52.5%), fatigue (25.4%), anemia (23.7%), thrombocytopenia (23.7%), neutropenia (22.0%), and hypoalbuminemia (22.0%). Most adverse events were grade I or II. Grade III adverse events included leukopenia (5.1%), diarrhea (5.1%), thrombocytopenia (3.4%), fatigue (1.7%), neutropenia (1.7%), loss of appetite (1.7%), hand-foot skin reaction (1.7%), and atrial fibrillation (1.7%). Grade IV adverse events included leukopenia (5.1%), myelosuppression (3.4%), erythropenia (3.4%), and neutropenia (1.7%) (Table 2). Confirmed immune-related adverse events were reactive cutaneous capillary endothelial proliferation and immune enteritis, with incidence of 8.5% and 1.7%, respectively. Other suspected

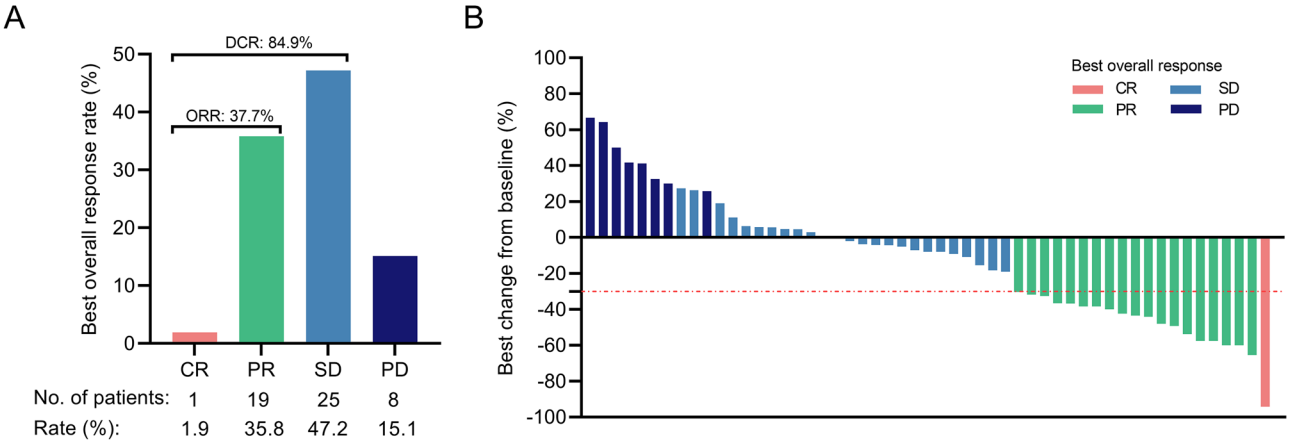

Fig. 2 The best overall response rate and target lesion diameter change from baseline. Best overall response rate (**A**) and best target lesion diameter change from baseline (**B**) in advanced or metastatic ESCC patients receiving CAM combined with apatinib plus IRT

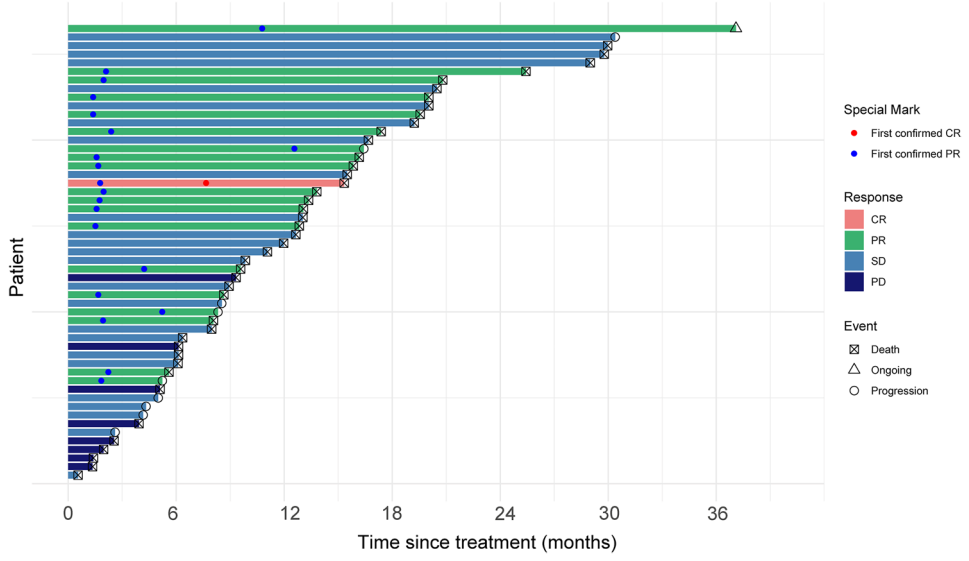

Fig. 3 Swimmer plot of patient prognosis

immune-related adverse events include fatigue, loss of appetite, increased TBIL, diarrhea, increased AST, increased ALT, and increased Cr. Due to the lack of documentation on how many of these adverse events were immune-related, the accurate incidence was unavailable (Table 2).

Evaluation of radiomic feature reproducibility

The reproducibility of radiomic feature extraction was assessed based on intra- and inter-observer agreement. The intra-observer ICC for the two measurements obtained by Reader A ranged from 0.847 to 0.952, while the inter-observer ICC between the two readers ranged from 0.774 to 0.893. These results indicated a high level of reproducibility for feature extraction both within and between observers. Consequently, all final results were based on measurements obtained by Reader A.

Radiomic feature extraction

A total of 1874 radiomic features were extracted from three-dimensional region of interest (ROI) images of esophageal cancer patients (Fig. 5A). The original features included 14 shape features, 18 first-order features, and 75 s-order (texture) features [including 24 Gy level co-occurrence matrix (GLCM) features, 14 Gy level dependence matrix features, 16 Gy level run length matrix (GLRLM) features, 16 Gy level size zone matrix features, and 5 neighborhood gray tone difference matrix (NGTDM) features]. The original CT images were filtered via wavelet, Laplacian-Gaussian, square, square root, logarithm, exponential, gradient filters, and Local Binary Pattern 2D/3D to generate higher-order statistics. High-pass (H) and low-pass (L) wavelet filters were applied to decompose the three-dimensional images, resulting in eight decomposition types: HHH, LLL, HHL,

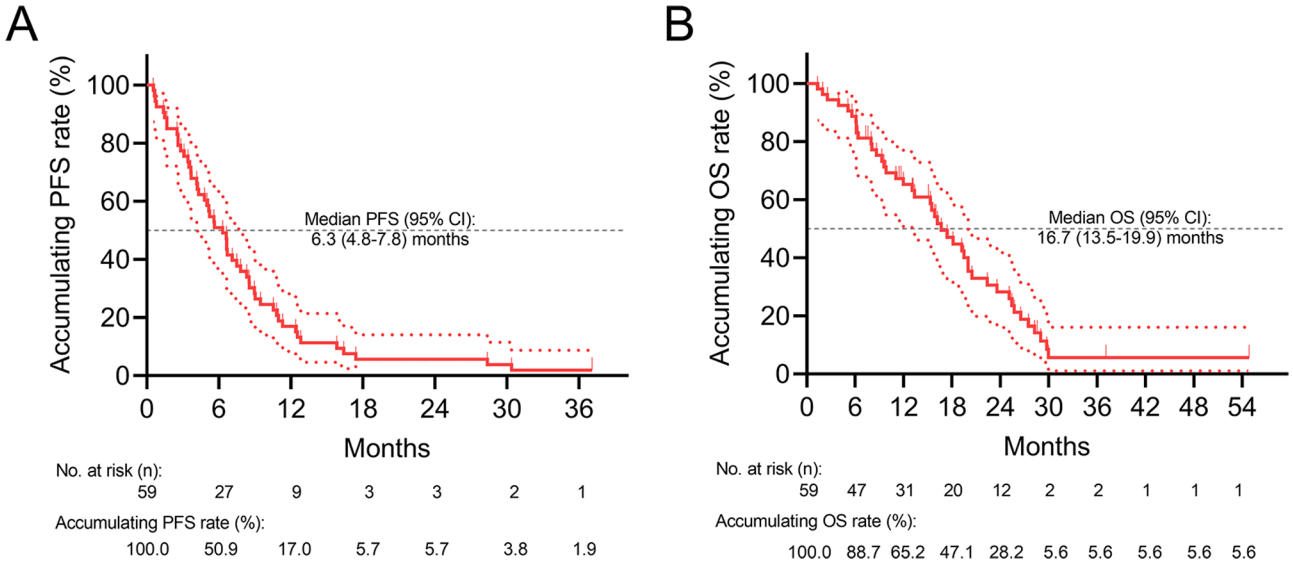

Fig. 4 PFS and OS. PFS (**A**) and OS (**B**) in advanced or metastatic ESCC patients receiving CAM combined with apatinib plus IRT

HLL, LHH, LHL, LLH, and HLH. Additionally, Local Binary Pattern 3D (LBP-3D) was applied in three orientations (Lbp-3D-k, Lbp-3D-m1, and Lbp-3D-m2) to resample the images. Consequently, the total number of radiomic features reached 1874, calculated as [(18 + 75) × 19 + 18 + 75 + 14 = 1,874]. After excluding features with a Pearson correlation coefficient absolute value ≥ 0.9, 313 features remained. Using LASSO Cox regression for dimensionality reduction, six radiomic features were ultimately selected (Figs. 5B-D).

Calculation of the rad-score

The selected features were weighted according to their respective coefficients derived from the LASSO model, and the Rad score was calculated via the following formula: Rad score=-0.512744195224548 *A_exponential_firstorder_90Percentile

+ 0.4324847868685487 *A_log-sigma-3-0-mm-3D_firstorder_Minimum

-0.4119442998802703*A_log-sigma-3-0-mm-3D_glcm_Correlation

+ 0.7475398962597095*A_wavelet-HLH_glszm_ZoneEntropy

-0.3735699541777159*A_wavelet-HLL_glszm_GrayLevelNonUniformityNormalized

-0.6918076857064893*A_wavelet-LHH_firstorder_Kurtosis

The cutoff value for the Rad score, determined via X-tile software, was − 0.5274497362077936. On the basis of this cutoff, patients were classified into high-risk and low-risk groups. Kaplan-Meier survival analysis revealed that OS in the low-risk group was significantly greater than that in the high-risk group ($P < 0.001$) (Figs. 5E-F).

Selection of clinical and radiomic features

Univariate and multivariate Cox proportional hazards models were used to identify significant clinical and radiomic features. Multivariate analysis of clinical features revealed that lactic dehydrogenase (LDH) [$P = 0.013$, hazard ratio (HR): 6.780, 95% CI: 1.500–30.800] and indirect bilirubin (IBIL) ($P = 0.012$, HR: 39.590, 95% CI: 2.220–704.000) were independent risk factors influencing patient prognosis (Table 3; Fig. 6A). For radiomic features, multivariate analysis indicated that A_exponential_firstorder_90Percentile ($P = 0.006$, HR: 0.009, 95% CI: 0.017–0.499), A_wavelet-HLH_glszm_ZoneEntropy ($P = 0.008$, HR: 3.870, 95% CI: 1.420–10.600), and A_wavelet-LHH_firstorder_Kurtosis ($P = 0.028$, HR: 0.100, 95% CI: 0.013–0.780) were associated with patient prognosis (Fig. 6B). In the combined model, the selected radiomic and clinical features were analyzed together in a multivariate Cox model. This analysis identified A_exponential_firstorder_90Percentile ($P = 0.023$, HR: 0.000, 95% CI: 0.000-0.398), A_wavelet-HLH_glszm_ZoneEntropy ($P = 0.019$, HR: 26.450, 95% CI: 1.730–404.000), and A_wavelet-LHH_firstorder_Kurtosis ($P = 0.016$, HR: 0.020, 95% CI: 0.001–0.486) as key radiomic features, along with clinical features, AST ($P = 0.045$, HR: 45370.81, 95% CI: 1.290–1.59 × 10^9) and IBIL ($P = 0.049$, HR: 1177.16, 95% CI: 1.03–1.35 × 10^6) as optimal predictors (Fig. 6C).

Model construction and evaluation

Three nomograms were developed to estimate the 1-year OS of patients based on the results of multivariate Cox regression analysis, utilizing clinical features (Fig. 6D), radiomic features (Fig. 6E), and combined clinical and radiomic features (Fig. 6F). The C-index was calculated for each model to assess the consistency between the

Table 2 Adverse events

Adverse events, *n* (%)	Any grade	Grade I	Grade II	Grade III	Grade IV
Leukopenia	31 (52.5)	11 (18.6)	14 (23.7)	3 (5.1)	3 (5.1)
Fatigue	15 (25.4)	12 (20.3)	2 (3.4)	1 (1.7)	0 (0.0)
Anemia	14 (23.7)	10 (16.9)	4 (6.8)	0 (0.0)	0 (0.0)
Thrombocytopenia	14 (23.7)	8 (13.6)	4 (6.8)	2 (3.4)	0 (0.0)
Neutropenia	13 (22.0)	6 (10.2)	5 (8.5)	1 (1.7)	1 (1.7)
Hypoalbuminemia	13 (22.0)	13 (22.0)	0 (0.0)	0 (0.0)	0 (0.0)
Myelosuppression	12 (20.3)	1 (1.7)	9 (15.3)	0 (0.0)	2 (3.4)
Loss of appetite	10 (16.9)	6 (10.2)	3 (5.1)	1 (1.7)	0 (0.0)
Erythropenia	10 (16.9)	5 (8.5)	3 (5.1)	0 (0.0)	2 (3.4)
Digestive tract reaction	8 (13.6)	6 (10.2)	2 (3.4)	0 (0.0)	0 (0.0)
Increased TBIL	8 (13.6)	6 (10.2)	2 (3.4)	0 (0.0)	0 (0.0)
Diarrhea	8 (13.6)	3 (5.1)	2 (3.4)	3 (5.1)	0 (0.0)
Liver dysfunction	7 (11.9)	4 (6.8)	3 (5.1)	0 (0.0)	0 (0.0)
Increased AST	6 (10.2)	4 (6.8)	2 (3.4)	0 (0.0)	0 (0.0)
RCCEP	5 (8.5)	5 (8.5)	0 (0.0)	0 (0.0)	0 (0.0)
Increased ALT	5 (8.5)	4 (6.8)	1 (1.7)	0 (0.0)	0 (0.0)
Lymphopenia	5 (8.5)	4 (6.8)	1 (1.7)	0 (0.0)	0 (0.0)
Weight loss	5 (8.5)	4 (6.8)	1 (1.7)	0 (0.0)	0 (0.0)
Increased blood pressure	4 (6.8)	2 (3.4)	2 (3.4)	0 (0.0)	0 (0.0)
Hand-foot skin reaction	4 (6.8)	2 (3.4)	1 (1.7)	1 (1.7)	0 (0.0)
Nausea and vomiting	3 (5.1)	1 (1.7)	2 (3.4)	0 (0.0)	0 (0.0)
Increased Cr	3 (5.1)	3 (5.1)	0 (0.0)	0 (0.0)	0 (0.0)
Hypocalcemia	2 (3.4)	2 (3.4)	0 (0.0)	0 (0.0)	0 (0.0)
Hypothyroidism	2 (3.4)	1 (1.7)	1 (1.7)	0 (0.0)	0 (0.0)
Fever	2 (3.4)	2 (3.4)	0 (0.0)	0 (0.0)	0 (0.0)
Sore throat	1 (1.7)	1 (1.7)	0 (0.0)	0 (0.0)	0 (0.0)
Gastrointestinal bleeding	2 (3.4)	0 (0.0)	2 (3.4)	0 (0.0)	0 (0.0)
Hemoptysis	1 (1.7)	1 (1.7)	0 (0.0)	0 (0.0)	0 (0.0)
Oral mucosal inflammation	1 (1.7)	0 (0.0)	1 (1.7)	0 (0.0)	0 (0.0)
Immune enteritis	1 (1.7)	0 (0.0)	1 (1.7)	0 (0.0)	0 (0.0)
Pain	1 (1.7)	0 (0.0)	1 (1.7)	0 (0.0)	0 (0.0)
Atrial fibrillation	1 (1.7)	0 (0.0)	0 (0.0)	1 (1.7)	0 (0.0)

TBIL, total bilirubin; AST, aspartate aminotransferase; RCCEP, reactive cutaneous capillary endothelial proliferation; ALT, alanine aminotransferase; Cr, creatinine

nomogram-predicted and observed survival outcomes. The C-indices for the clinical model, radiomics model, and combined model were 0.666, 0.881, and 0.914, respectively (Figs. 6G-I), indicating a high level of agreement between predicted and actual survival outcomes for all models. ROC curve analysis demonstrated that the clinical model had an area under the curve (AUC) of 0.679 (95% CI: 0.551–0.807) (Fig. 6J), while the radiomics model achieved an AUC of 0.979 (95% CI: 0.930–1.000) (Fig. 6K), and the combined model also reached an AUC of 0.979 (95% CI: 0.930–1.000) (Fig. 6L). The DCA of three predictive models revealed that the radiomics model and combined model exhibited satisfactory net benefits; however, due to the small sample size, the "all" line was not able to be generated for the clinical model, which limited the ability to fully assess the clinical utility of this model (Figs. 6M-O). Overall, the combined model exhibited the highest predictive value for 1-year OS in patients.

Discussion

Two previous studies explored the efficacy of CAM plus apatinib as a second-line treatment in advanced ESCC patients [17, 18]. One study reported that CAM plus apatinib as a second-line treatment achieved an ORR of 34.6% in advanced ESCC patients [17]. Another study indicated that CAM plus apatinib as a second-line treatment resulted in an ORR and a DCR of 10.2% and 69.4%, respectively, in advanced ESCC patients [18]. In the present study, CAM combined with apatinib plus IRT as second-line treatment achieved an ORR and DCR of 37.7% and 84.9%, respectively, in advanced or metastatic ESCC patients. Our findings were comparable to those of a previous study [17]. However, the ORR (37.7% vs. 10.2%) and DCR (84.9% vs. 69.4%) in this study were obviously higher than those reported in other previous studies [18]. We speculated that different prior treatments might contribute to the inconsistent findings. In our study, no patients had a history of immunotherapy, but the previous study enrolled advanced ESCC patients who were previously treated with immune checkpoint inhibitors [18]. Compared with other second-line treatments, such as chemotherapy (ORR: 6.4-22.0%, DCR: 41.8-62.0%) [19–21], tislelizumab (ORR: 20.4%, DCR: 47.0%) [19], CAM (ORR: 20.2%, DCR: 44.7%) [20], and apatinib (ORR: 7.5-24.2%, DCR: 65.0-74.2%) [8, 10], the treatment response to CAM combined with apatinib plus IRT seemed to be higher suggesting the potential of this combined therapy as a second-line treatment for advanced or metastatic ESCC patients. Moreover, we provided evidence that the median (IQR) time of first achieving PR was 1.9 (1.6–2.4) months in patients who achieved PR, and the first time of achieving PR and CR were 1.8 and 7.7 months, respectively, in patients who achieved CR. Our findings revealed that CAM combined with apatinib plus IRT possessed a rapid onset of action in advanced or metastatic ESCC patients.

The combination of CAM and apatinib as a second-line treatment has the potential to prolong survival in patients with various cancers [22–26]. Regarding advanced ESCC, a previous study reported that the median PFS and OS were 6.8 and 15.8 months, respectively, in advanced ESCC patients receiving CAM plus apatinib as second-line treatment [17]. Another study reported that second-line CAM plus apatinib resulted in a median PFS and OS of 4.6 and 7.5 months, respectively, in advanced ESCC

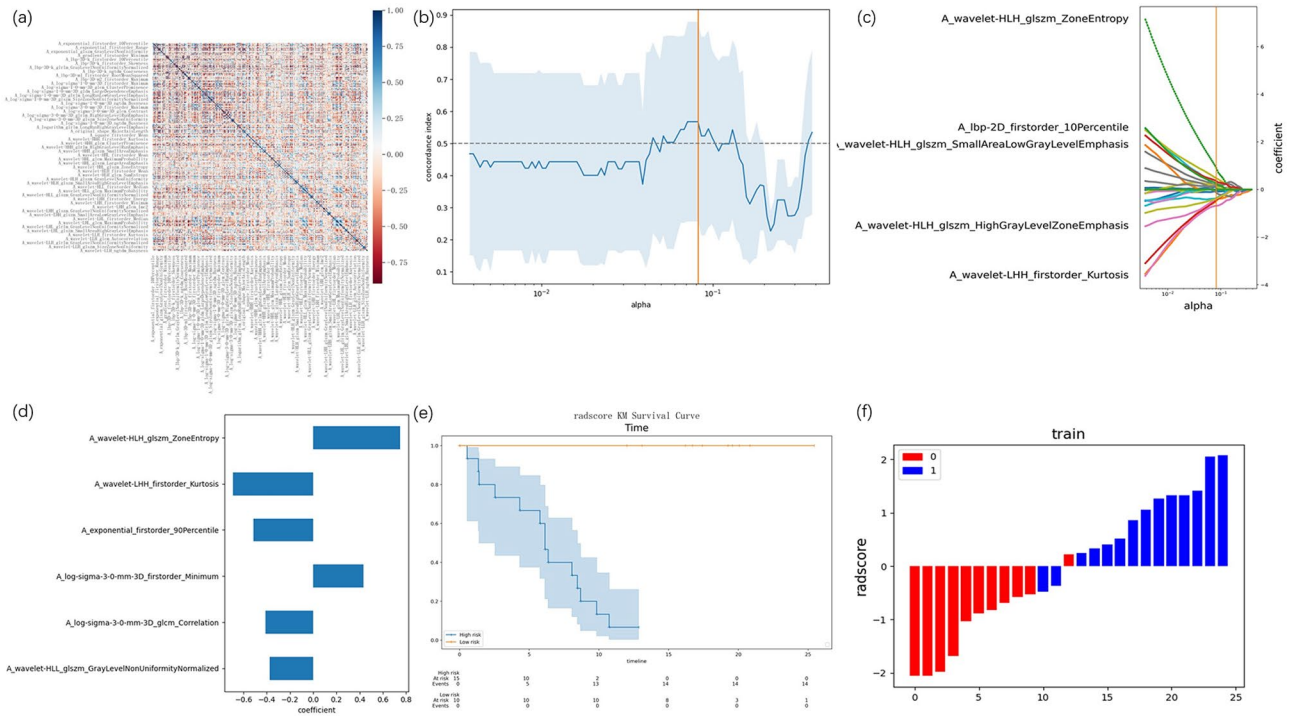

Fig. 5 LASSO-based radiomic feature selection process and preliminary evaluation of the radiomics model. Correlation analysis of radiomic features (**A**). LASSO model accuracy score plot (**B**). LASSO path diagram (**C**). LASSO model feature weight plot (**D**). Kaplan-Meier survival analysis between low-risk and high-risk groups (**E**). Radiomics scores for each patient in the training group (**F**)

patients [18]. In this study, we found that the median PFS and OS were 6.3 and 16.7 months, respectively, in advanced or metastatic ESCC patients receiving CAM combined with apatinib plus IRT as second-line treatment. Our findings were in accordance with those of a previous study [17] but inconsistent with those of another study that included patients who were previously treated with immune checkpoint inhibitors [18]. Therefore, patients without previous immune checkpoint inhibitors might benefit more from CAM combined with apatinib plus IRT. According to other previous studies, the median PFS and OS were 1.9–3.4 and 6.2–8.4 months, respectively, in patients receiving second-line chemotherapy [19–21]; 1.6 months and 8.6 months, respectively, in patients receiving second-line tislelizumab [19]; 1.9 and 8.3 months, respectively, in patients receiving second-line CAM [20]; and 3.8 and 5.8-7.0 months, respectively, in patients receiving second-line apatinib [8, 10]. Compared with these second-line treatments, CAM combined with apatinib plus IRT as second-line treatment could prolong survival in advanced or metastatic ESCC patients.

Common adverse events after CAM monotherapy included reactive cutaneous capillary endothelial proliferation, hypothyroidism, anemia, and leukopenia in advanced ESCC patients [20]. Regarding apatinib, common adverse events included hand-foot syndrome, hypertension, proteinuria, hepatic injury, and fatigue in advanced ESCC patients [8]. Common adverse events after chemotherapy (including IRT) were leukopenia, neutropenia, and anemia [19]. In this study, we found that the common adverse events were leukopenia, fatigue, anemia, thrombocytopenia, neutropenia, and hypoalbuminemia, most of which were mild and tolerable. The adverse events of this combination regimen were consistent with those of individual drugs [8, 19, 20]. Meanwhile, the incidence of grade III/IV adverse events was 20.3% in this study, which was lower than CAM combined with apatinib plus chemotherapy as the first-line treatment (90.0%) [13]. Overall, our findings disclosed that CAM combined with apatinib plus IRT as the second-line treatment was tolerable for advanced or metastatic ESCC patients.

Moreover, we also established three nomograms to predict the 1-year OS based on the outcomes of multivariate Cox analyses in advanced or metastatic ESCC patients receiving CAM combined with apatinib plus IRT as second-line treatment. The function of these nomograms was to provide a comprehensive and individualized prognostic assessment for patients. The clinical nomogram offered a prediction tool based on easily accessible clinical data, while the radiomic nomogram captured detailed tumor characteristics from imaging. The combined nomogram integrated both clinical and radiomic features

Table 3 Univariate and multivariate Cox analysis for the clinical model

	Univariate analysis			Multiplicity analysis		
	P value	HR	95%CI	*P* value	HR	95%CI
Gender						
Male vs. female	0.125	0.357	0.096 ~ 1.332			
Age						
<60 vs. ≥60	0.420	0.618	0.192 ~ 1.990			
BMI						
BMI<25 vs. BMI ≥ 25	0.192	0.258	0.033 ~ 1.981			
ECOG PS						
ECOG = 0 vs. ECOG = 1	0.387	0.041	0.000 ~ 57.381			
Tumor location						
Cervical vs. thoracic and abdominal	0.976	1.016	0.343 ~ 3.013			
Pathological grading						
Well vs. others	0.684	0.909	0.573 ~ 1.441			
Number of organs with metastases						
Organ = 1 vs. Organs>1	0.074	1.616	0.954 ~ 2.735			
History of radiotherapy						
No vs. Yes	0.120	2.322	0.803 ~ 6.714			
History of primary lesion surgery						
No vs. Yes	0.600	1.330	0.458 ~ 3.858			
History of targeted drug therapy						
NO vs. YES	0.663	0.636	0.083 ~ 4.877			
Maximum change in target lesion diameter						
<0% vs.≥0%	0.934	1.066	0.238 ~ 4.770			
CEA (ng/mL)						
CEA <5 vs. CEA ≥ 5	0.348	1.854	0.511 ~ 6.730			
AST (IU/L)						
AST < 40 vs. AST ≥ 37	**0.026**	23.475	1.469 ~ 375.680			
ALT (IU/L)						
ALT < 41 vs. ALT ≥ 41	0.054	22.060	0.001 ~ 501,589			
LDH (IU/L)						
LDH < 250 vs. LDH ≥ 250	**0.006**	6.387	1.682 ~ 24.250	**0.013**	6.780	1.500 ~ 30.800
ALP (IU/L)						
ALP < 129 vs. ALP ≥ 129	0.469	1.742	0.388 ~ 7.824			
UA (umol/L)						
UA < 428 vs. UA ≥ 428	0.583	0.565	0.071 ~ 4.334			
ALB (g/L)						
ALB < 40 vs. ALB ≥ 40	0.697	0.810	0.280 ~ 2.340			
DBIL (umol/L)						
DBIL < 6 vs. DBIL ≥ 6	0.688	0.770	0.214 ~ 2.768			
IBIL (umol/L)						
IBIL < 17 vs. IBIL ≥ 17	**0.046**	11.490	1.042 ~ 126.760	**0.012**	39.590	2.220 ~ 704.0

CI: confidence interval; HR: hazard ratio; BMI, body mass index; ECOG PS, Eastern Cooperative Oncology Group Performance Status; CEA, carcinoembryonic antigen; AST, aspartate aminotransferase; ALT, alanine aminotransferase; LDH, lactic dehydrogenase; ALP, alkaline phosphate; UA, uric acid; ALB, albumin; DBIL, direct bilirubin; IBIL, indirect bilirubin

to enhance prediction accuracy and offer a more holistic view of patient outcomes. It was found that the combined model (A_exponential_firstorder_90Percentile, A_wavelet-HLH_glszm_ZoneEntropy, and A_wavelet-LHH_firstorder_Kurtosis, AST, and IBIL) had an excellent ability to predict the 1-year OS in advanced or metastatic ESCC patients with an AUC of 0.979. Our findings provided support for clinical treatment decision-making and aided in identifying patients who were most likely to benefit from CAM combined with apatinib plus IRT as second-line treatment. In clinical practice, clinicians could apply this model by inputting clinical (AST and IBIL) and radiomic (A_exponential_firstorder_90Percentile, A_wavelet-HLH_glszm_ZoneEntropy, and A_wavelet-LHH_firstorder_Kurtosis) parameters into the nomogram. This process will yield a total score, which can then be used to estimate the patient's 1-year OS probability. Based on this prediction, clinicians can better tailor

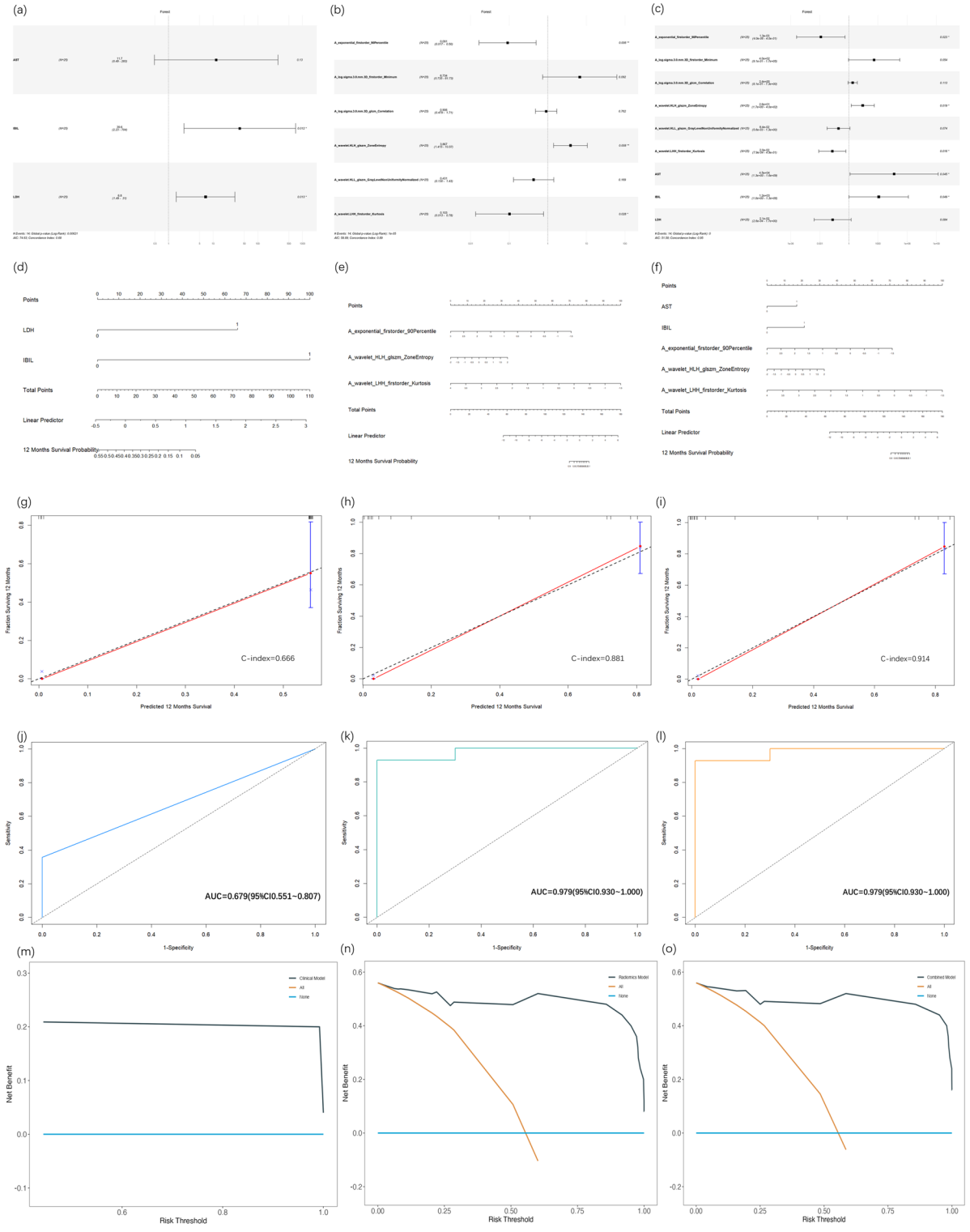

Fig. 6 Predictive values for the models. Forest plot of Cox multivariate analysis for the clinical model (**A**). Forest plot of Cox multivariate analysis for the radiomics model (**B**). Forest plot of Cox multivariate analysis for the combined model (**C**). Nomogram for estimating 1-year OS utilizing clinical features (**D**). Nomogram for estimating 1-year OS utilizing radiomic features (**E**). Nomogram for estimating 1-year OS utilizing combined clinical and radiomic features (**F**). Calibration curve for the clinical model (**G**). Calibration curve for the radiomics model (**H**). Calibration curve for the combined model (**I**). ROC curves for the clinical model (**J**). ROC curves for the radiomics model (**K**). ROC curves for the combined model (**L**). DCA of the clinical model (**M**). DCA of the radiomics model (**N**). DCA of the combined model (**O**)

treatment strategies for each patient, thereby improving patients' prognosis. It should be clarified that while this combined model shows promising predictive ability, its practical application in clinical settings requires further validation to ensure reliability and utility.

This study contained two complementary sections: the former was a clinical trial that explored the efficacy and safety of CAM combined with apatinib plus IRT as a second-line treatment in advanced or metastatic ESCC patients; the latter was the clinical model construction, which aimed to predict the survival of advanced or metastatic ESCC patients receiving the combined regimen. These two sections provided a comprehensive evaluation of the combination therapy: the clinical trial disclosed its efficacy and safety, while the clinical models offered a tool for predicting patient prognosis and optimizing treatment selection.

This study contained several limitations. (1) The sample size of this study was relatively small, which limited the statistical power. (2) This was a single-arm study, which lacked a control group for direct comparison. Further randomized, controlled trials were required to validate the efficacy of CAM combined with apatinib and IRT as second-line treatment in advanced or metastatic ESCC patients. (3) This study was conducted in China, which limited the generalizability of our findings. (4) In this study, biopsy samples were used to diagnose ESCC. However, sequencing data were not included. Collecting sequencing data was important to elucidate the mechanisms underlying the efficacy of CAM combined with apatinib plus IRT. Therefore, further studies should incorporate such data to explore this aspect.

Conclusions

In conclusion, CAM combined with apatinib plus IRT as a second-line treatment results in satisfactory efficacy with manageable safety profiles in advanced or metastatic ESCC patients. Clinically, this combined regimen may enrich second-line treatments in advanced or metastatic ESCC patients. Moreover, the model that combines clinical and radiomic features has the optimal ability to predict the survival of advanced or metastatic ESCC patients.

Acknowledgements
Not applicable.

Author contributions
Yifu He and Shusheng Wu contributed to the study conception and design. Material preparation, data collection and analysis were performed by Shusheng Wu, Jiayu Niu, Gang Wang, Lihong Ke, Mengge Li, Ying Yan, Huijun Xu, Xiaoxiu Hu, Wenju Chen, Huiqin Luo, Bing Hu, Huimin Li, Lulu Cao. The first draft of the manuscript was written by Shusheng Wu, Yifu He commented on previous versions of the manuscript. All authors reviewed and approved the final version of the manuscript.

Funding
This research was funded by the Health Commission of Anhui Province Scientific Research Project (AHWJ2023BAc10031 and AHWJ2023A30183); Anhui Provincial Clinical Key Specialty Construction Project Funding (2023sjlczdzk02), and Fundamental Research Funds for the Central Universities (WK9110000172).

Data availability
The datasets used and/or analyzed during the current study are available from the corresponding author on reasonable request.

Declarations

Ethics approval and consent to participate
The study was approved by the Medical Ethics Committee of the First Affiliated Hospital of USTC West District (Approval Number: Lunshen 2019 No. 24) and was prospectively registered in the China Clinical Trial Registry (ChiCTR2000028857) on January 5, 2020. Informed consent was obtained from all patients.

Consent for publication
Not applicable.

Competing interests
The authors declare no competing interests.

Author details
[1]Department of Medical Oncology, Division of Life Sciences and Medicine, The First Affiliated Hospital of USTC, University of Science and Technology of China, No. 107 Huanhu Road East, Shushan District, Hefei, Anhui 230031, China
[2]Department of Medical Oncology, Anhui Provincial Cancer Hospital, Hefei, Anhui 230031, China
[3]Graduate School, Wannan Medical College, Wuhu, Anhui 241002, China
[4]Department of Medical Oncology, Anqing Municipal Hospital, Anqing, Anhui 246000, China

Received: 26 January 2025 / Accepted: 23 April 2025
Published online: 09 May 2025

References

1. Sheikh M, Roshandel G, McCormack V, Malekzadeh R. Current Status and Future Prospects for Esophageal Cancer. Cancers (Basel). 2023;15(3).
2. Puhr HC, Prager GW, Ilhan-Mutlu A. How we treat esophageal squamous cell carcinoma. ESMO Open. 2023;8(1):100789.
3. Morgan E, Soerjomataram I, Rumgay H, Coleman HG, Thrift AP, Vignat J, Laversanne M, Ferlay J, Arnold M. The Global Landscape of Esophageal Squamous Cell Carcinoma and Esophageal Adenocarcinoma Incidence and Mortality in 2020 and Projections to 2040: New Estimates From GLOBOCAN 2020. Gastroenterology. 2022;163(3):649–58. e2.
4. He S, Xu J, Liu X, Zhen Y. Advances and challenges in the treatment of esophageal cancer. Acta Pharm Sin B. 2021;11(11):3379–92.
5. Yang YM, Hong P, Xu WW, He QY, Li B. Advances in targeted therapy for esophageal cancer. Signal Transduct Target Ther. 2020;5(1):229.
6. Yang H, Li X, Yang W. Advances in targeted therapy and immunotherapy for esophageal cancer. Chin Med J (Engl). 2023;136(16):1910–22.
7. Zhang H. Apatinib for molecular targeted therapy in tumor. Drug Des Devel Ther. 2015;9:6075–81.
8. Li J, Wang L. Efficacy and safety of apatinib treatment for advanced esophageal squamous cell carcinoma. OncoTargets therapy. 2017;10:3965–69.
9. Zhao J, Lei J, Yu J, Zhang C, Song X, Zhang N, Wang Y, Zhang S. Clinical efficacy and safety of apatinib combined with S-1 in advanced esophageal squamous cell carcinoma. Invest New Drugs. 2020;38(2):500–06.
10. Chu L, Chen Y, Liu Q, Liang F, Wang S, Liu Q, Yu H, Wu X, Zhang J, Deng J, et al. A Phase II Study of Apatinib in Patients with Chemotherapy-Refractory Esophageal Squamous Cell Carcinoma (ESO-Shanghai 11). Oncologist. 2021;26(6):e925–35.
11. Li H, Huang H, Zhang T, Feng H, Wang S, Zhang Y, Ji X, Cheng X, Zhao R. Apatinib: A Novel Antiangiogenic Drug in Monotherapy or Combination

Immunotherapy for Digestive System Malignancies. Front Immunol. 2022;13:937307.
12. Baba Y, Nomoto D, Okadome K, Ishimoto T, Iwatsuki M, Miyamoto Y, Yoshida N, Baba H. Tumor immune microenvironment and immune checkpoint inhibitors in esophageal squamous cell carcinoma. Cancer Sci. 2020;111(9):3132–41.
13. Zhang B, Qi L, Wang X, Xu J, Liu Y, Mu L, Wang X, Bai L, Huang J. Phase II clinical trial using camrelizumab combined with apatinib and chemotherapy as the first-line treatment of advanced esophageal squamous cell carcinoma. Cancer Commun (Lond). 2020;40(12):711–20.
14. Wilk AM, Kozlowska E, Borys D, D'Amico A, Fujarewicz K, Gorczewska I, Debosz-Suwinska I, Suwinski R, Smieja J, Swierniak A. Radiomic signature accurately predicts the risk of metastatic dissemination in late-stage non-small cell lung cancer. Transl Lung Cancer Res. 2023;12(7):1372–83.
15. Liu H, Cui Y, Chang C, Zhou Z, Zhang Y, Ma C, Yin Y, Wang R. Development and validation of a (18)F-FDG PET/CT radiomics nomogram for predicting progression free survival in locally advanced cervical cancer: a retrospective multicenter study. BMC Cancer. 2024;24(1):150.
16. Cui Y, Li Z, Xiang M, Han D, Yin Y, Ma C. Machine learning models predict overall survival and progression free survival of non-surgical esophageal cancer patients with chemoradiotherapy based on CT image radiomics signatures. Radiat Oncol. 2022;17(1):212.
17. Meng X, Wu T, Hong Y, Fan Q, Ren Z, Guo Y, Yang X, Shi P, Yang J, Yin X, et al. Camrelizumab plus apatinib as second-line treatment for advanced oesophageal squamous cell carcinoma (CAP 02): a single-arm, open-label, phase 2 trial. Lancet Gastroenterol Hepatol. 2022;7(3):245–53.
18. Meng X, Wang J, Xia J, Wu T, Luo Z, Hong Y, Lu P, Guo Y, Ji Y, Zhang M, et al. Efficacy and safety of camrelizumab plus apatinib in patients with advanced esophageal squamous cell carcinoma previously treated with immune checkpoint inhibitors (CAP 02 Re-challenge): A single-arm, phase II study. Eur J Cancer. 2024;212:114328.
19. Shen L, Kato K, Kim SB, Ajani JA, Zhao K, He Z, Yu X, Shu Y, Luo Q, Wang J, et al. Tislelizumab Versus Chemotherapy as Second-Line Treatment for Advanced or Metastatic Esophageal Squamous Cell Carcinoma (RATIONALE-302): A Randomized Phase III Study. J Clin oncology: official J Am Soc Clin Oncol. 2022;40(26):3065–76.
20. Huang J, Xu J, Chen Y, Zhuang W, Zhang Y, Chen Z, Chen J, Zhang H, Niu Z, Fan Q, et al. Camrelizumab versus investigator's choice of chemotherapy as second-line therapy for advanced or metastatic oesophageal squamous cell carcinoma (ESCORT): a multicentre, randomised, open-label, phase 3 study. Lancet Oncol. 2020;21(6):832–42.
21. Kato K, Cho BC, Takahashi M, Okada M, Lin CY, Chin K, Kadowaki S, Ahn MJ, Hamamoto Y, Doki Y, et al. Nivolumab versus chemotherapy in patients with advanced oesophageal squamous cell carcinoma refractory or intolerant to previous chemotherapy (ATTRACTION-3): a multicentre, randomised, open-label, phase 3 trial. Lancet Oncol. 2019;20(11):1506–17.
22. Yao Y, Wang Y, Du Y, Jiang F, Liang H, Bi M, Xie H, Peng W, Pan Y. Efficacy and safety of second-line camrelizumab combined with apatinib and chemotherapy in patients with advanced lung adenocarcinoma: A prospective, open-label, multicentric study. Int Immunopharmacol. 2023;125(Pt B):111147.
23. Xu J, Shen J, Gu S, Zhang Y, Wu L, Wu J, Shao G, Zhang Y, Xu L, Yin T, et al. Camrelizumab in Combination with Apatinib in Patients with Advanced Hepatocellular Carcinoma (RESCUE): A Nonrandomized, Open-label, Phase II Trial. Clin Cancer Res. 2021;27(4):1003–11.
24. Gao G, Zhao J, Ren S, Wang Y, Chen G, Chen J, Gu K, Guo R, Pan Y, Wang Q, et al. Efficacy and safety of camrelizumab plus apatinib as second-line treatment for advanced squamous non-small cell lung cancer. Ann Transl Med. 2022;10(8):441.
25. Jing C, Wang J, Zhu M, Bai Z, Zhao B, Zhang J, Yin J, Yang X, Liu Z, Zhang Z, et al. Camrelizumab combined with apatinib and S-1 as second-line treatment for patients with advanced gastric or gastroesophageal junction adenocarcinoma: a phase 2, single-arm, prospective study. Cancer Immunol Immunother. 2022;71(11):2597–608.
26. Mei K, Qin S, Chen Z, Liu Y, Wang L, Zou J. Camrelizumab in combination with apatinib in second-line or above therapy for advanced primary liver cancer: cohort A report in a multicenter phase Ib/II trial. J Immunother Cancer. 2021;9(3).

Publisher's note